

FERMILAB-Pub-95/304-A  
DART-HEP-95/05  
Sept. 1995

# Nonperturbative effects on nucleation

Marcelo Gleiser

*Department of Physics and Astronomy, Dartmouth College,  
Hanover, NH 03755, USA  
email: gleiser@peterpan.dartmouth.edu*

Andrew F. Heckler

*NASA/Fermilab Astrophysics Center, Fermi National Accelerator Laboratory,  
Batavia, IL 60510, USA  
email: aheckler@fnas04.fnal.gov*

## Abstract

A nonperturbative correction to the thermal nucleation rate of critical bubbles in a first order phase transition is estimated. The correction originates from large-amplitude fluctuations which may be present before the transition occurs. Using a simple model of a scalar field in a double-well potential, we present a method to obtain a corrected potential which incorporates the free-energy density available from large-amplitude fluctuations, which is not included in the usual perturbative calculation. For weaker phase transitions, the nucleation rate can be much larger than the rate calculated via perturbation theory. As an application of our method, we show how nonperturbative corrections can both qualitatively and quantitatively explain anomalously high nucleation rates observed in 2-d numerical simulations.

Although the simplest first order phase transitions are characterized by a discontinuous jump of a scalar order parameter between two distinct phases, they do not all proceed in the same way [1]. For very strong first order phase transitions, where the free-energy barrier between the phases is large, the transition is initiated by the nucleation of critical-sized bubbles of the new phase in the background of the metastable (*e.g.*, super-cooled) old phase. By definition, these critical bubbles are just large enough to overcome their surface tension and grow, eventually converting the whole medium to the new phase. The large barrier between the two phases suppresses large-amplitude thermal fluctuations of the order parameter; an initial metastable state is well-defined, as no fraction of the volume is in the new phase before the transition occurs. In this case, the metastable phase can be regarded as “homogeneous”, as only very small-amplitude thermal fluctuations are present. This is the situation described by Langer’s theory of homogeneous nucleation [2], or, in the context of relativistic quantum field theories, by the work of Coleman and Callan [3].

Besides the decay of the “near-homogeneous” metastable state described by nucleation theory, one can investigate the evolution of an unstable initial state which is characterized by considerable phase mixing. Within the context of condensed matter systems, this situation corresponds to a quench within the unstable “spinodal” region of the two-phase diagram. In this case, the two phases separate by the mechanism known as “spinodal decomposition”; small-amplitude, long-wavelength fluctuations grow exponentially fast, forming domains of the two phases which will eventually coarsen, as the system approaches its final equilibrium state.

In this letter we will address the dynamics of phase transitions characterized by an initial state which lies within the “grey zone” between homogeneous nucleation and spinodal decomposition. Looking at the whole “spectrum” of first order phase transitions, from very strong to very weak, it is clear that the amount of phase-mixing of the initial state will strongly influence the subsequent dynamics of the transition. However, the standard method of calculating the nucleation rate employs Gaussian perturbation theory, which is valid only for small amplitude fluctuations [4]. For strong transitions this approximation is valid. But for weaker transitions, large amplitude fluctuations are more abundant, and can have an important effect. Our goal is to present an approximate method by which the presence of large-amplitude fluctuations is consistently incorporated into the calculation of nucleation rates. Thus, we are implicitly assuming that we are close enough to the regime described by homogeneous nucleation that we can still distinguish between the two low-temperature phases.

Large-amplitude thermal fluctuations will be modelled by the so-called sub-critical bubble method [5]. Recent results [6] have shown that modelling the dominant fluctuations by sub-critical bubbles is in excellent agreement with 3-d simulations [7]. The model utilizes the fact that along with the nucleation of critical bubbles in the meta-stable phase, smaller size, though still large amplitude, “sub-critical” bubbles will also be nucleated (and in much greater number because they have a lower free energy). These bubbles by definition will always shrink and eventually disappear, but there will always be some non-zero equilibrium number density  $n_{\text{sb}}$  at a given temperature. Their presence may lead to large corrections on nucleation rates.

To begin, let us consider the standard model of a phase transition, in which the order

parameter is a real scalar field  $\phi$ , which has a quartic double-well potential of the form

$$V(\phi) = \frac{1}{2}m^2\phi^2 - \frac{1}{6}g\phi^3 + \frac{h}{24}\phi^4. \quad (1)$$

This potential has two minima, one at  $\phi = 0$  and at  $\phi = \phi_+$ , which represent the two phases of the system. It can be thought of as the homogeneous part of a typical phenomenological Ginzburg-Landau coarse-grained free-energy density (the cubic term can always be made into a linear term), or as some effective potential where additional degrees of freedom coupled to  $\phi$  have been integrated out. Our analysis will be purely classical, valid for  $T \gg m$ , where  $m$  is the mass of the low-energy mesonic excitations in the associated quantum theory. All relevant field configurations contain many quanta.

We would like to incorporate the free-energy density associated with large-amplitude, nonperturbative fluctuations into the computation of the decay rate. In the spirit of the renormalization group approach, this should be equivalent to an effective “coarse-graining” of the classical potential; averaging over these large-amplitude fluctuations will lead to a shift in the background free-energy density and decay barrier, which in principle can be translated into a change in the bare couplings of the model. We can understand how to estimate the effective coarse-graining by first studying the thin-wall limit of critical bubble nucleation.

In the standard theory, which neglects phase mixing, the nucleation rate  $\Gamma$  is proportional to  $e^{-F_{\text{cb}}/T}$ , where  $F_{\text{cb}}$  is free energy needed to form a critical bubble in the metastable background. For an arbitrary thin-walled spherical bubble of radius  $R$  and amplitude  $\phi_{\text{thin}} \lesssim \phi_+$ , where thin-walled means the radius  $R$  is much greater than the bubble wall thickness, the free energy of the bubble takes the well-known form [8]

$$F_{\text{thin}}(R) = 4\pi R^2\sigma - \frac{4\pi}{3}R^3\Delta V. \quad (2)$$

This formula has a simple physical interpretation. The first term is the energy it costs to form the bubble wall, where  $\sigma \equiv \frac{1}{2} \int dr (\partial\phi/\partial r)^2$  is the surface tension. The second term is the energy “gained” by converting a spherical volume of the metastable phase into the lower energy phase. Therefore,  $\Delta V$  is defined as the difference in free-energy density between the background medium and the bubble’s interior. Since  $\phi_{\text{thin}} \lesssim \phi_+$ , for a homogeneous background (metastable) we can write,

$$\Delta V_0 = V(0) - V(\phi_+), \quad (3)$$

where we have explicitly used the subscript 0 to stress that this is for the case with no phase mixing.

If there is significant phase mixing in the background metastable state, its free-energy density is no longer  $V(0)$ . One must also account for the free-energy density of the non-perturbative, large-amplitude fluctuations. Since there is no formal way of deriving this contribution outside improved perturbative schemes, we propose to estimate the corrections to the background free-energy density by following another route. We start by writing

$$\text{free-energy density of metastable state} = V(0) + \mathcal{F}_{\text{sc}}, \quad (4)$$

where  $\mathcal{F}_{\text{sc}}$  is the nonperturbative contribution to the free-energy density due to the large amplitude fluctuations, which we assume can be modelled by subcritical bubbles. We will calculate  $\mathcal{F}_{\text{sc}}$  further below.

We thus define the effective free-energy difference  $\Delta V_{\text{cg}}$ , which includes corrections due to phase mixing, as

$$\Delta V_{\text{cg}} = \Delta V_0 + \mathcal{F}_{\text{sc}} \quad (5)$$

which is the sum of the free-energy difference calculated in the standard way [eq. (2)], and the “extra” free-energy density due to the presence of subcritical bubbles. Henceforth, the subscript ‘cg’ will stand for “coarse-grained”.

We note that while we have made a correction to  $\Delta V$ , we have not made any correction to the surface tension  $\sigma$ . Since we are considering the thin-wall limit, as long as  $\langle \phi \rangle$  is small, which is true if subcritical bubbles do not occupy a large fraction of space, the correction to  $\sigma$  will be subdominant. [Note that the presence of subcritical bubbles may shift  $\langle \phi \rangle$  by roughly  $\sum_i e^{-F_i/T} \phi_i$ , where  $\phi_i$  is the amplitude of a given fluctuation, and  $F_i$  its associated free energy.] Thus, the arguments here give a lower bound on the magnitude of the corrections. Later on, both volume and surface corrections will be automatically included in the calculation.

Since a critical size bubble is defined as the bubble for which all forces on the bubble wall cancel, *i.e.*  $\partial F / \partial R|_{R_{\text{cb}}} = 0$ , we can now use eq. (2) to obtain the free energy needed to form a thin-wall critical bubble in a background with subcritical bubbles

$$F_{\text{cb}} = \frac{2\pi}{3} R_{\text{cb}}^3 (\Delta V_0 + \mathcal{F}_{\text{sc}}) = \frac{16\pi}{3} \frac{\sigma^3}{(\Delta V_0 + \mathcal{F}_{\text{sc}})^2} \quad (6)$$

and the radius of the critical bubble is

$$R_{\text{cb}} = \frac{2\sigma}{\Delta V_0 + \mathcal{F}_{\text{sc}}}. \quad (7)$$

Equations (6) and (7) warrant several comments. First, in the limit of a very strong phase transition, subcritical bubbles are suppressed ( $\mathcal{F}_{\text{sc}} \rightarrow 0$ ), and both  $F_{\text{cb}}$  and  $R_{\text{cb}}$  approach the standard expressions for the free energy and radius of a critical bubble in a homogeneous background. Second, notice that  $\mathcal{F}_{\text{sc}}$  acts in the same way as the free-energy difference  $\Delta V_0$ . The presence of subcritical bubbles is equivalent to extra free energy in the medium, which enhances the nucleation of critical bubbles. In particular, for potentials near degeneracy such that  $\Delta V_0 \lesssim \mathcal{F}_{\text{sc}}$ , the nucleation rate of critical bubbles  $\Gamma \sim e^{-F_{\text{cb}}/T}$ , can be *much* greater than in the case ignoring the presence of subcritical bubbles.

Finally, notice that as  $\Delta V_0 \rightarrow 0$ , neither the critical-bubble energy nor its radius become infinite. For temperature-dependent potentials which (ignoring the corrections from subcritical bubbles) are degenerate at the critical temperature  $T_c$ , the nucleation rate  $\Gamma \sim e^{-F_{\text{cb}}/T_c}$  is finite. In fact, the nucleation rate of critical bubbles may be non-zero even *above* the critical temperature (again, using the uncorrected expression for the potential). This is a testable prediction of our method which, of course, is sensitive to the equilibrium number-density of subcritical bubbles.

This final comment suggests an important point. Since for degenerate potentials (temperature dependent or not) no critical bubbles should be nucleated, taking into account subcritical bubbles must lead to a change in the coarse-grained free-energy density (or potential) describing the transition. Thus, it should be possible to translate the “extra” free energy available in the system due to the presence of subcritical bubbles in the background into a corrected potential for the scalar order parameter. We will write this corrected potential as  $V_{\text{cg}}(\phi)$ .

The standard coarse-grained free energy is calculated by integrating out the short wavelength modes (usually up to the correlation length) from the partition function of the system, and is approximated by the familiar form [9]

$$F_{\text{cg}} = \int d^3r \left( \frac{1}{2}(\nabla\phi)^2 + V_{\text{cg}}(\phi) \right) . \quad (8)$$

How do we estimate  $V_{\text{cg}}$ ? One way is to simply constrain it to be consistent with the thin wall limit. That is, as  $V_{\text{cg}}(\phi)$  approaches degeneracy (*i.e.*  $\Delta V_{\text{cg}}(\phi) \rightarrow 0$ ), it must obey the thin wall limit of eq. (5). Note that with a simple rescaling, the potential of eq. (1) can be written in terms of one free parameter. Thus, the thin wall constraint can be used to express the corrected value of this parameter in terms of  $\mathcal{F}_{\text{sc}}$  in appropriate units. The free energy of the critical bubble is then obtained by finding the bounce solution to the equation of motion  $\nabla^2\phi - dV_{\text{cg}}(\phi)/d\phi = 0$  by the usual shooting method, and substituting this solution into eq. (8).

Therefore, in order to determine  $V_{\text{cg}}$ , we must first calculate the free-energy density  $\mathcal{F}_{\text{sc}}$  of the subcritical bubbles. As a first step, we follow the work of Ref. [6], to obtain the equilibrium number density  $n_{\text{sb}}$  of subcritical bubbles. If we define the distribution function  $f \equiv \partial^2 n_{\text{sb}} / \partial R \partial \phi_A$ , then  $f(R, \phi_A, t) dR d\phi_A$  is the number density of bubbles with radius between  $R$  and  $R + dR$  and amplitude between  $\phi_A$  and  $\phi_A + d\phi_A$  at time  $t$ . It satisfies the Boltzmann equation,

$$\frac{\partial f(R, \phi_A, t)}{\partial t} = -|v| \frac{\partial f}{\partial R} + (1 - \gamma) G_{0 \rightarrow +} - f \mathcal{V} G_{\text{Therm}} - \gamma G_{+ \rightarrow 0}. \quad (9)$$

The first term on the RHS is the shrinking term (note that  $v = \partial R / \partial t$  is negative), the second term is the nucleation term where  $G$  is the nucleation distribution function, which is defined by  $\Gamma = \int dR d\phi G$ , and  $\Gamma_{0 \rightarrow +}$  is the nucleation rate per unit volume of subcritical bubbles from the “0” phase (the initial phase) to the “+” phase. The division of the system into two phases depends on the particular application at hand, as will be clear in the example below. By the Gibb’s distribution,  $G_{0 \rightarrow +} = A e^{-F_{\text{sb}}(R, \phi_A)/T}$ , where  $A$  is a constant independent of  $R$  and  $\phi$ .

The factor  $\gamma$  is defined as the fraction of volume in the “+” phase, and is obtained by summing over subcritical bubbles of all amplitudes within this phase. The third term is a phenomenological thermal destruction term (see work by Gelmini and Gleiser in Ref. [5]), where  $\mathcal{V}$  is the volume of a bubble of radius  $R$ , and  $G_{\text{Therm}} = aT/\mathcal{V}$ , where  $a$  is a constant. The fourth term is the inverse nucleation term. For more details about this Boltzmann equation, see Ref. [6], which has improved upon the work of Gelmini and Gleiser (Ref. [5]).

The free energy of the subcritical bubbles is determined by modelling them as Gaussian fluctuations with amplitude  $\phi_A$  and radius  $R$ ,

$$\phi_{\text{sc}}(r) = \phi_A e^{-r^2/R^2}. \quad (10)$$

The free energy of a given configuration can then be found by using the general formula,

$$F_{\text{sb}} = \int d^3r \left( \frac{1}{2} (\nabla \phi_{\text{sc}})^2 + V(\phi_{\text{sc}}) \right). \quad (11)$$

Although this approach only includes one particular shape out of all possible field configurations, the agreement between theory and numerical experiments indicates that the Gaussian profile is an adequate *ansatz* for the dominant large-amplitude thermal fluctuations.

The equilibrium number density of subcritical bubbles is found by solving eq. (9) with  $\partial f/\partial t = 0$ , imposing the physical boundary condition  $f(r \rightarrow \infty) = 0$ . Once we know the distribution function and free energy for a bubble of a given radius  $R$  and amplitude  $\phi_A$ , we can estimate the total energy density of the Gaussian subcritical bubbles, summed over all relevant radii and amplitudes. We can write, in general,

$$\mathcal{F}_{\text{sc}} \approx \int_{\phi_{\text{min}}}^{\infty} \int_{R_{\text{min}}}^{R_{\text{max}}} F_{\text{sb}} \frac{\partial^2 n_{\text{sb}}}{\partial R \partial \phi_A} dR d\phi_A, \quad (12)$$

where  $\phi_{\text{min}}$  defines the lowest amplitude within the “+” phase, typically (but not necessarily) taken to be the maximum of the double-well potential.  $R_{\text{min}}$  is the smallest radius for the subcritical bubbles, compatible with the coarse-graining scale. For example, it can be a lattice cut-off in numerical simulations, or the mean-field correlation length in continuum models. As for  $R_{\text{max}}$ , it is natural to choose it to be the critical bubble radius.

As an application of the above method, we will investigate nucleation rates in the context of a 2-d model for which accurate numerical results are available [10]. This will allow us to compare the results obtained by incorporating subcritical bubbles into the calculation of the decay barrier with the results from the numerical simulations.

The 2-d scalar potential  $V(\phi)$  is given in eq. (1). Following the rescaling of Ref. [10], the potential can be written in terms of one dimensionless parameter  $\lambda \equiv m^2 h/g^2$ ,

$$V(\phi) = \frac{1}{2} \phi^2 - \frac{1}{6} \phi^3 + \frac{\lambda}{24} \phi^4. \quad (13)$$

This double-well potential is degenerate when  $\lambda = 1/3$ , and the second minimum is lower than the first when  $\lambda < 1/3$ .

As argued before, we find the new coarse-grained potential  $V_{\text{cg}}$  (or, equivalently,  $\lambda_{\text{cg}}$ ) by constraining it to agree with the thin wall limit. Simple algebra from eqs. (5) and (13) yields, to first order in the deviation from degeneracy,

$$\lambda_{\text{cg}} = \lambda - \frac{\tilde{\mathcal{F}}_{\text{sc}}}{54} \quad (14)$$

where  $\tilde{\mathcal{F}}_{\text{sc}} = \frac{g^2}{m^6} \mathcal{F}_{\text{sc}}$  is the dimensionless free-energy density in subcritical bubbles. The new potential  $V_{\text{cg}}$  is then used to find the bounce solution and the free energy of the critical bubble.

The calculation of  $\mathcal{F}_{\text{sc}}$  in two dimensions is fairly straightforward. Close to the thin wall limit (*i.e.*,  $G_{0 \rightarrow +} \approx G_{+ \rightarrow 0} \equiv G$ ), one can analytically solve the equilibrium Boltzmann equation for the density distribution function, obtaining  $f(R, \phi_A, T) = (1 - 2\gamma)W_T(R, \phi_A)$ , where ( $v \equiv |v|$ )

$$W_T(R, \phi_A) = \frac{(A/v)}{2} \exp \left[ -\frac{\alpha}{T} + RT(a/v) + \frac{(a/v)^2 T^3}{4\beta} \right] \sqrt{\frac{\pi T}{\beta}} \left\{ 1 - \text{erf} \left[ \sqrt{\frac{\beta}{T}} \left( R + \frac{(a/v)T^2}{2\beta^2} \right) \right] \right\}, \quad (15)$$

and we wrote the free energy of a given subcritical configuration as  $F_{\text{sb}} \equiv \alpha + \beta R^2$ , with  $\alpha = \pi\phi_A^2/2$ , and  $\beta = \alpha \left( \frac{1}{2} - \frac{1}{9}\phi_A + \frac{\lambda}{48}\phi_A^2 \right)$ . The fraction of the volume occupied by subcritical bubbles is then,

$$\gamma(\phi_{\text{max}}, R_{\text{min}}, R_{\text{max}}) = \frac{I_T(\phi_{\text{max}}, R_{\text{min}}, R_{\text{max}})}{[1 + 2I_T(\phi_{\text{max}}, R_{\text{min}}, R_{\text{max}})]}, \quad (16)$$

where,  $I_T = \int_{\phi_{\text{max}}}^{\infty} \int_{R_{\text{min}}}^{R_{\text{max}}} \pi r^2 W_T dr d\phi$ . The radial integration can be done analytically, although the result is not particularly illuminating. The integral over amplitudes must be done numerically. We then substitute  $f(R, \phi_A, T)$  and  $\gamma$  into eq. (12) to finally find  $\mathcal{F}_{\text{sc}}(\lambda, T, A/v, a/v)$ .

In order to illustrate the effect of subcritical bubbles on the nucleation barrier, in Figure 1 we compare the value for the barrier obtained with and without the corrections, as a function of  $\lambda$ , for constant values of the temperature. The temperatures are chosen to be within the range used in the 2-d simulation. The constant  $A$  was fixed at  $A = 0.02$ , consistent with the measurements of Ref. [10]. Notice that the presence of subcritical bubbles greatly decreases the barrier as the potential approaches degeneracy ( $\lambda \rightarrow 1/3$ ). However, for small temperatures  $T < 10m^4/g^2$ , the correction becomes negligible.

In Figure 2 we show that the calculation of the nucleation barrier including the effects of subcritical bubbles is consistent with data from lattice simulations, whereas the standard calculation overestimates the barrier by a large margin. In fact, the inclusion of subcritical bubbles provides a reasonable explanation for the anomalously high nucleation rates observed in the simulations close to degeneracy. The error bars are from the numerical measurements of the barrier; for larger values of  $\lambda$ , higher temperatures had to be used to attain nucleation, increasing the error in the barrier measurements. However, we note that even with the large error bars, the data is inconsistent with the theoretical predictions for the barriers, while the corrected barrier values fall within the error bars for a wide range of parameters. We note that data from 1-d simulations also show the same behavior as the data in Figure 2 [10]. Simulations in 3-d are in progress, and will enable us to test this method in more detail.

Finally, we note that the inclusion of nonperturbative corrections through the definition of an effective, “coarse-grained”, coupling may have several consequences not only to the nucleation rate of first order transitions, but also to their dynamics. Clearly, once we have a corrected potential, quantities such as the critical temperature, the amount of super-cooling, the bubble-wall velocities, and the completion time for the transition will change. This opens up several possible applications of this method, from laboratory studies of nucleation to cosmological phase transitions.

We thank S. Dodelson, J. Frieman, E.W. Kolb, A. Stebbins, and E.J. Weinberg for stimulating discussions. MG was partially supported by the National Science Foundation through a Presidential Faculty Fellows Award (PHY-9453431), and by NASA (NAGW-4270). He thanks the Nasa/Fermilab Astrophysics Center for their kind hospitality during part of this work. AFH was supported in part by the DOE and by NASA (NAG5-2788) at Fermilab.

## References

- [1] J. D. Gunton, M. San Miguel and P. S. Sahni, in *Phase Transitions and Critical Phenomena*, **Vol. 8**, Ed. C. Domb and J. L. Lebowitz (Academic Press, London, 1983).
- [2] J. S. Langer, Ann. Phys. (NY) **41**, 108 (1967); *ibid.* **54**, 258 (1969).
- [3] S. Coleman, Phys. Rev. **D15**, 2929 (1977); C. Callan and S. Coleman, Phys. Rev. **D16**, 1762 (1977).
- [4] P. Ramond, *Field Theory: A Modern Primer*, 2nd Ed. (Addison-Wesley, New York, 1990).
- [5] M. Gleiser, E. W. Kolb, and R. Watkins, Nucl. Phys. **B364**, 411 (1991); G. Gelmini and M. Gleiser, Nucl. Phys. **B419**, 129 (1994); M. Gleiser and E. W. Kolb, Phys. Rev. Lett. **69**, 1304 (1992); N. Tetradis, Z. Phys. **C57**, 331 (1993).
- [6] M. Gleiser, A.F. Heckler, and E.W. Kolb, *in progress*. (Preliminary results of this collaboration can be found in M. Gleiser, hep-ph/9507312).
- [7] J.D. Borrill and M. Gleiser, Phys. Rev. **D51**, 4111 (1995).
- [8] A. Linde, Nucl. Phys. **B216**, 421 (1983); [Erratum: **B223**, 544 (1983)].
- [9] J.S. Langer, Physica **73**, 61 (1974).
- [10] M. Alford and M. Gleiser, Phys. Rev. **D48**, 2838 (1993). 1-d simulations were performed by M. Alford, H. Feldman, and M. Gleiser, Phys. Rev. **D47** (RC), 2168 (1993).

## List of Figures

Figure 1. Comparison of the decay barrier as a function of  $\lambda$  with and without the inclusion of subcritical bubbles, at fixed temperatures.

Figure 2. Comparison between numerical data and theoretical predictions for the decay barrier with and without the inclusion of subcritical bubbles.

Figure 1

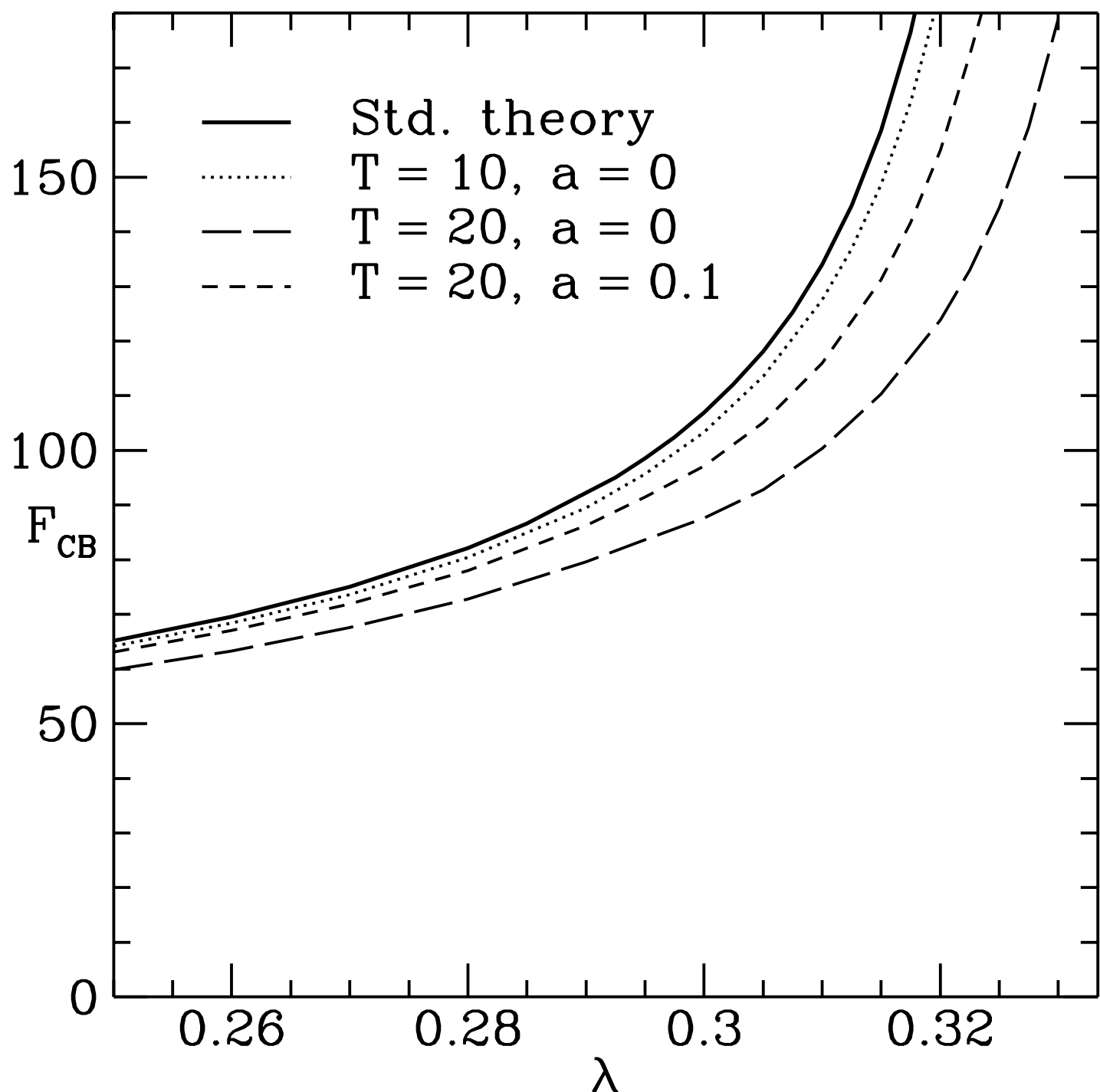


Figure 2

